Supplementary Information (SI) for RSC Applied Interfaces.

Supporting Information

Self-assembled Molecule Modified Nickel Oxide Surface for Air-Processed Blue Perovskite Light-Emitting Diodes

Jiandong Wu[1], Yujie Wang[1], Fankai Lin[1], Chaoran Ni[1], Shuhao Xiong[1], Miao Zhang[2], Hongyue Wang[1*], Hongqiang Wang[1*]

[1] State Key Laboratory of Solidification Processing, Center for Nano Energy Materials, School of Materials Science and Engineering, Northwestern Polytechnical University and Shaanxi Joint Laboratory of Graphene, Xi'an, 710072, China.

[2] Materials Institute of Atomic and Molecular Science, School of Physics & Information Science Shaanxi University of Science and Technology, Xi’an 710021, China.

Experimental section

X.1. Materials.

Lead bromide ($PbBr_2$, 99.999 %), cesium bromide (CsBr, 99.999 %), dimethyl sulfoxide (DMSO), isopropyl alcohol (IPA), Chlorobenzene (CB), lithium fluoride (LiF, 99.999 %), Triphenylphosphine oxide (TPPO) were purchased from Sigma-Aldrich. β-Alanine (>98 %) and (2-(3,6-Dibromo-9H-carbazol-9-yl)ethyl)phosphonic acid (Br-2PACz, >99%) were purchased from Tokyo Chemical Industry (TCI). Phenylethylammonium bromide (PEABr) was obtained from Xi'an Polymer Technology Corp. 2, 2', 2" -(1,3,5-Benzinetriyl)-tris(1 phenyl-1-Hbenzimidalzole) (TPBi, 99.5 %) was obtained from Luminescence Technology Corp. Molybdenum Trioxide (MoO_3) was purchased from Vizuchem Co., Ltd (Shanghai, China). Diethyl ether, acetone and anhydrous ethanol were purchased from Sinopharm Chemical Reagent Co., Ltd. Deionized water fabricated in the laboratory. All the chemicals were used without further purification.

X.2. Preparation of perovskite precursor solution.

The quasi-2D perovskite precursor solution $PEA_2(CsPbBr_3)_2PbBr_4$ was prepared by dispersing the CsBr (0.133 mmol), $PbBr_2$ (0.1 mmol), PEABr (0.067 mmol) and β-Alanine (0.05 mmol) into 1mL DMSO, and then stirring at 80 °C for 2h in a glovebox. The precursor was filtered using 0.22 μm polytetrafluoroethylene filters.

X.3 Device Fabrication.

ITO-coated glass substrates with a square resistance of 17 Ω/sq, purchased from Yingkou OPv Tech New EnergyCo., Ltd. The patterned ITO-coated glass substrates were first cleaned by sonicated detergent, deionized water, acetone, isopropyl alcohol, and ethanol in ultrasonic bath for 15 min each, and then dried by N_2 flow. Afterwards, the cleaned ITO substrates were treated by plasma for 15 min before use. We prepared the hole transport layers (HTLs), the perovskite layer, and the passivation layer in ambient air (T ≈ 21 °C, RH ≈ 20 %). The HTLs was constructed by spin-coating NiO_x (50μL) on the pre-treated ITO glass at 4000 r/min for 40 s, followed by annealing at 100 °C for 15 min; then plasma for 10 s and spin-coating Br-2PACz (40μL) upon the NiO_x film at 3000 r/min for 30 s, followed by annealing at 100 °C for 10 min. To deposit perovskite layer, the precursor solution (40 μL) was spin-coated at a speed of 3000 r/min for 70 s, during which 230 mL of diethyl ether was dropped on the wet perovskite film after 40 s of spin-coating, followed by a 4 min annealing at 70 °C on a hot plate. TPPO was then dissolved in CB solution (0.3 mg mL^{-1}) and spin-coated on perovskite at 7000 r/min, 40 s, served as the passivation layer. Finally, the samples were transferred into a thermal evaporator and completed by sequent vacuum deposition of 33.3 nm TPBi, 1.2 nm LiF, and 100 nm Al with a speed of 0.6, 0.1, and 3 Å s^{-1}, respectively. The performance of prepared PeLEDs devices were tested in a glovebox, including current density voltage curve, EL spectra, luminance, EQE, and operational lifetime.

X.4. Characterization.

The steady-state PL emission spectra were acquired using an Edinburgh (FLS 980) spectrometer (excitation wavelength: 365 nm). Absorption spectra were collected using the Perkin-Elmer Lambda 35 UV-vis-NIR spectrometer. Test time-resolved photoluminescence (TRPL) decay spectra of perovskite film using the HORIDA DeltaFlex lifetime system (400 nm blue LED excitation). Photoluminescence quantum yield (PLQY) tested by Hamamatsu's QY measurement system (C11347) with 365 nm ultraviolet excitation. The cross-sectional of the device were observed using an Tescan Clara GMH scanning electron microscopy (SEM) system. All the surface roughness and KPFM potential distribution images tested by Bruker Dimension Icon atomic force microscopy (AFM) in air. In-situ PL measurements were conducted using an Ocean

Optics' spectrometer equipped with 365 nm UV exciter. XPS and UPS spectra were acquired using a PHI 5000 Versa Probe, where UPS using a VG Scienta R4000 analyzer and a monochromatic He I light source. Contact angles measurements were collected on a Data physics OCA-20 contact-angle system in ambient air. The performance of PeLEDs was characterized in the emission area of 4 mm^2 in glovebox, including current density voltage curve, EL spectra, luminance, EQE, and operational lifetime (T50) of the devices using Keithley 2400 source meter equipped with a CDS2600 pectrometer (Labsphere Optics). The glue dispenser/spin coater (Brand-REESEEN, PvS-mini9) used in the lab are from Jiangyin J. Wanjia Technology Co., Ltd.

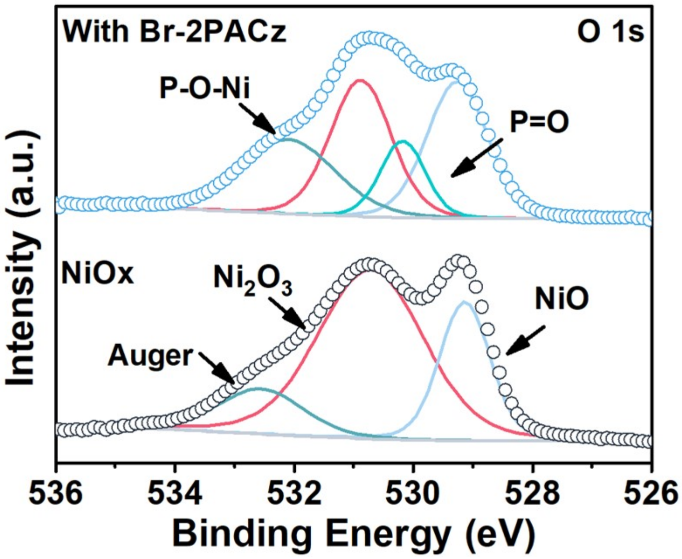

Figure S1. High-resolution XPS spectra of O 1s of the prepared substrates.

Table S1. The fitted proportion of Ni^{2+} and Ni^{3+} in NiO_x films with and without Br-2APCz.

Samples	Ni^{2+}/ Peak area	Ni^{2+}/ Proportion	Ni^{3+}/ Peak area	Ni^{3+}/ Proportion
NiO_x	105142	13.89%	270389	35.72%
With Br-2PACz	16104	15.36%	35212	34.23%

As shown in Table S1, the Ni^{3+} content in NiO_x film decreases from 35.72% to 34.23% after Br-2PACz modification, providing further evidence of the bonding interaction between Br-2PACz and NiO_x.

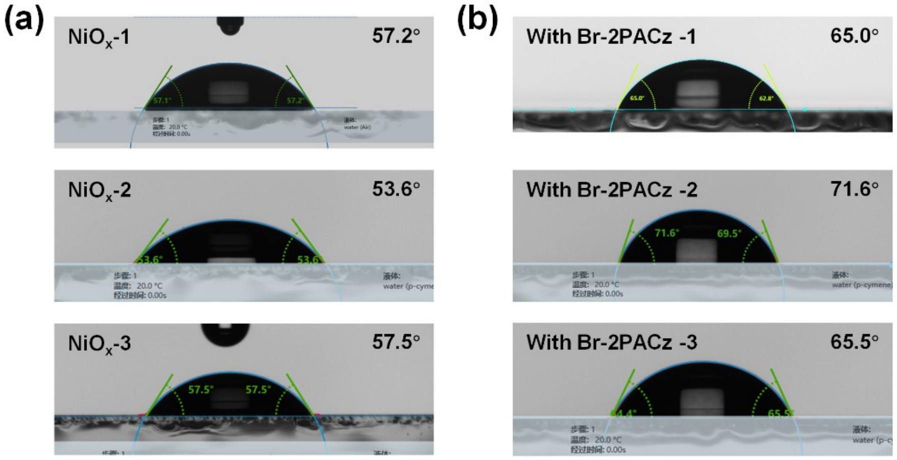

Figure S2. The water contact angle measurements of (a) NiO$_x$ and (b) Br-2PACz modified films.

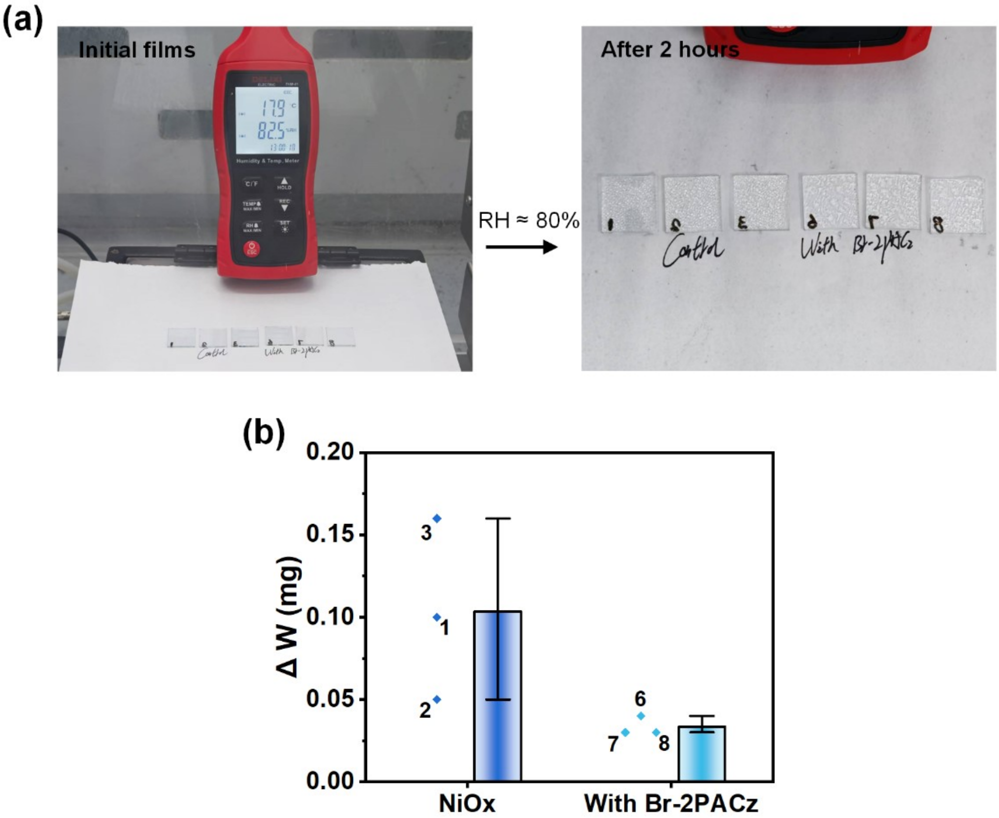

Figure S3. (a) Experimental analysis of the moisture adsorption for NiO$_x$ and Br-2PCAz modified substrates. (b) The statistical average water uptake of prepared samples.

Note S1. LaMer's law of crystallization kinetics.

According to LaMer curve and classical nucleation theory, the nucleation rate is governed by the critical Gibbs free energy (ΔGc), which can be regarded as the activation energy for initial nucleation and is used to describe the nucleation rate through an Arrhenius-type equation:

$$\frac{dN}{dt} = A\exp\left(-\frac{\Delta G_C}{k_B T}\right) \tag{1}$$

where t is time, N is the number of nuclei, dN/dt denotes the nucleation rate, A is the pre-exponential factor, k_B is the Boltzmann constant, and T is the absolute temperature. Meanwhile, the relationship between the critical Gibbs free energy and surface energy can be expressed as:

$$\Delta G_c = \frac{16\pi\gamma^3 v^2}{3(K_B^2 T^2 \ln S)^2} \tag{2}$$

where γ is the surface energy, v is the molar volume, and S represents the supersaturation ratio of the solution. Generally, a higher surface energy leads to an increased critical free energy, which in turn results in a lower nucleation rate and a reduced density of nucleation sites. In our study, the enhanced hydrophobicity of Br-2PACz-modified NiO_x surface indicates reduced surface energy, which in turn accelerated the nucleation and crystal growth rates, as confirmed by in-situ PL measurements (Figure 3g).

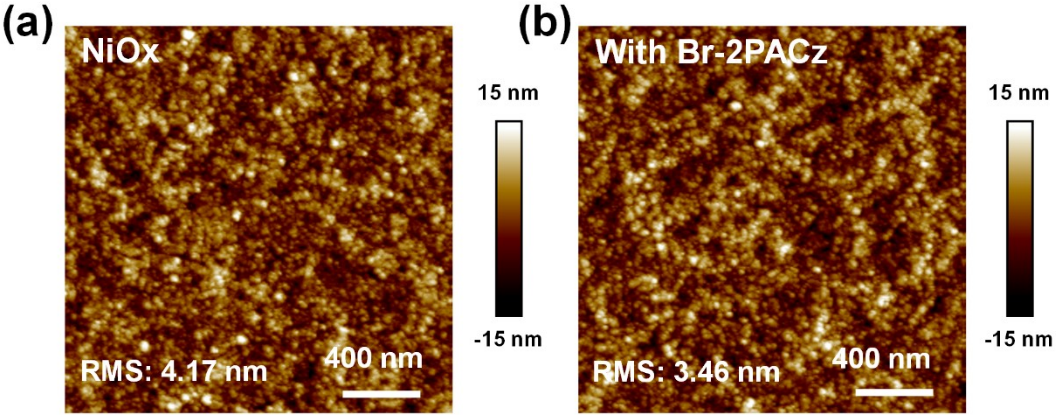

Figure S4. AFM images of the (a) NiO_x layer and after (b) Br-2PACz modification.

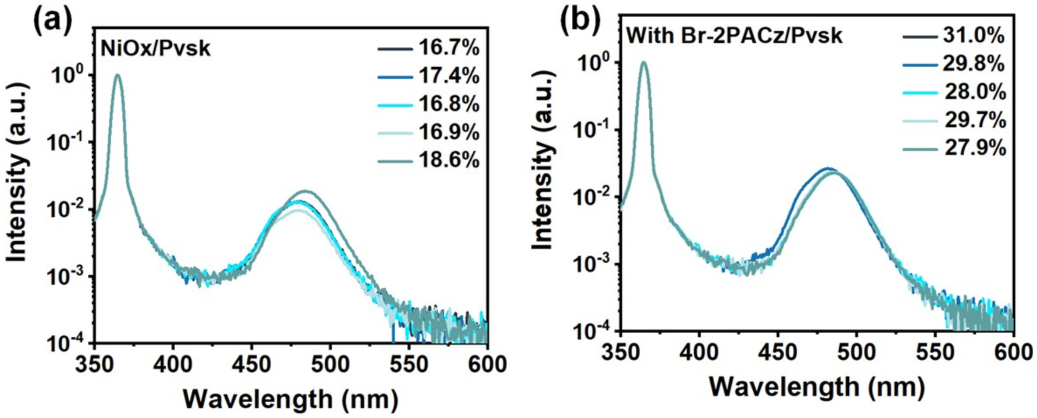

Figure S5. PLQY of air-processed perovskite films on (a) NiO_x and (b) Br-2PACz modified subtracts.

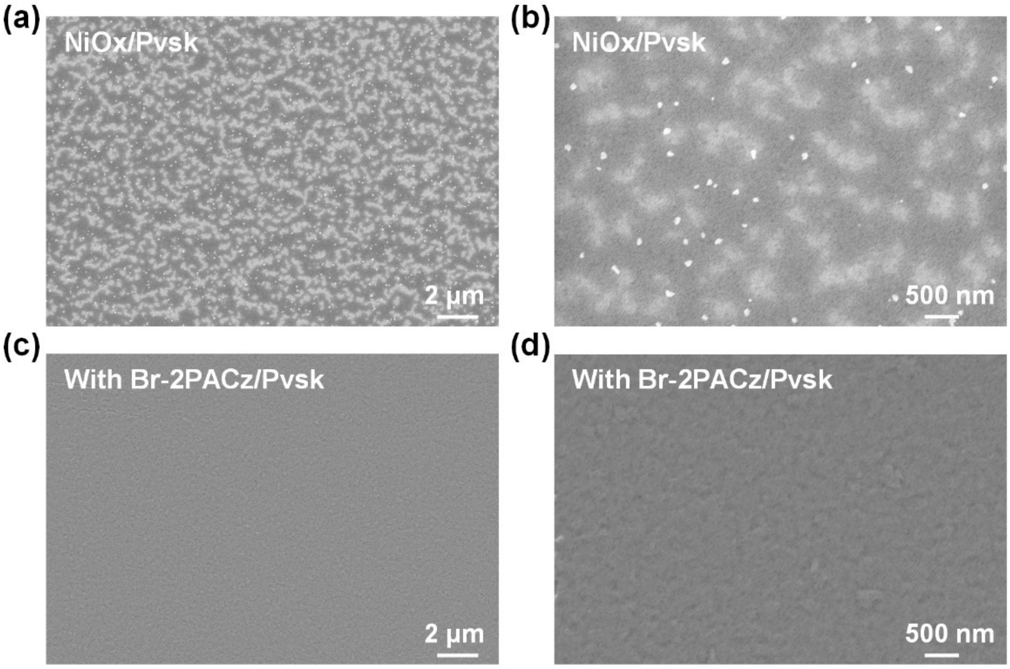

Figure S6. SEM images of perovskite films on the (a-b) NiO_x and (c-d) Br-2PACz modified substrates.

Table S2. The fitted carrier lifetime form TRPL of perovskite film on NiO_x and Br-2PACz modified substrates.

Parameters	NiO_x/perovskite	With Br-2PACz/perovskite
A_1 (%)	0.20	0.79
τ_1 (ns)	4.88	2.20
A_2 (%)	0.80	0.22
τ_2 (ns)	1.62	7.57
A_3 (%)	0.009	0.019
τ_3 (ns)	26.93	38.39
τ_{avg} (ns)	5.40	10.85

The TRPL curves fitted with tri-exponential function, $I(t)= I_0 + A_1 \exp(-t/\tau_1) + A_2 \exp(-t/\tau_2) + A_3 \exp(-t/\tau_3)$, where A_1, A_2 and A_3 are the amplitudes, τ_1, τ_2 and τ_3 represents the fast decay, middle decay and slow decay time refer to nonradiative recombination and radiative recombination, respectively. The τ_{avg} is calculate by the formula:

$$\tau_{avg} = \frac{A_1\tau_1^2 + A_2\tau_2^2 + A_3\tau_3^2}{A_1\tau_1 + A_2\tau_2 + A_3\tau_3}$$

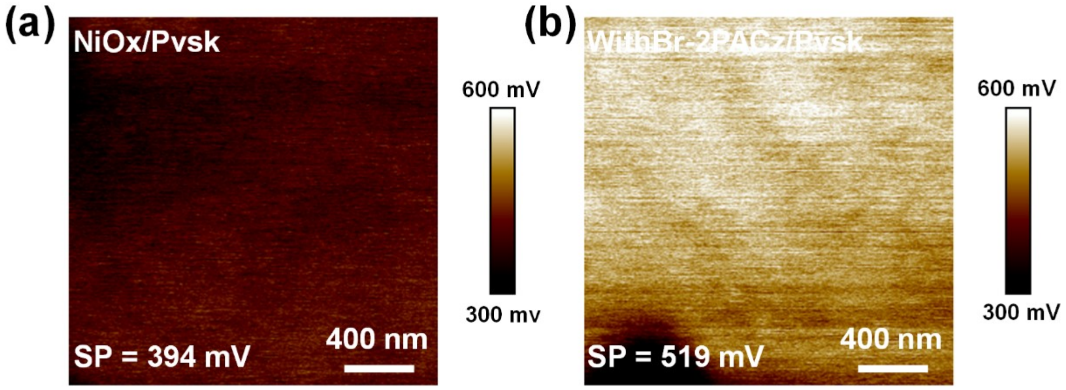

Figure S7. KPFM images of the perovskite film on (a) NiO_x layer and (b) Br-2PACz modified layer.

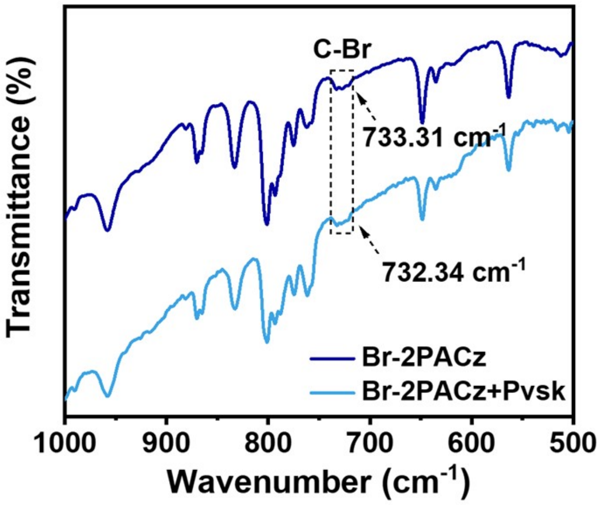

Figure S8. FT-IR spectra of Br-2PACz powder and the mixture of Br-2PACz and perovskite components of CsBr and $PbBr_2$.

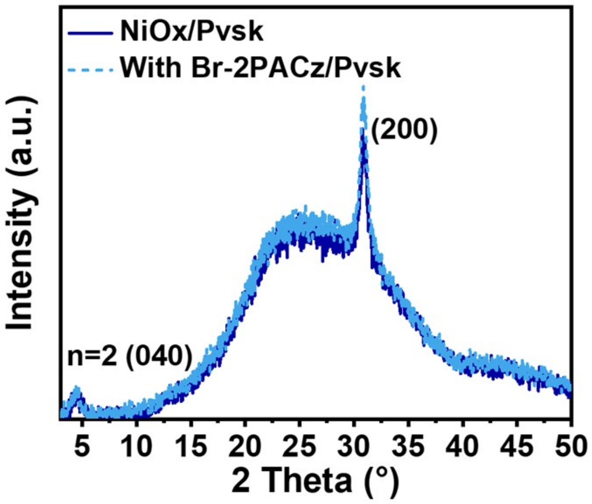

Figure S9. XRD patterns of perovskite film on both substrates.

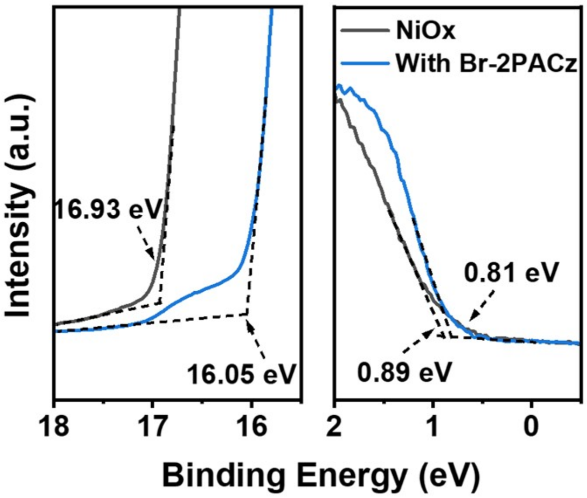

Figure S10. UPS spectra of the NiO_x layer and after Br-2PACz modification.

As shown in Figure S10, the cutoff energy (E_{cutoff}) and Fermi level (E_F) of NiO_x film are 16.93 eV and 0.89 eV, respectively. After modification with Br-2PACz, both energy levels exhibit a decrease, shifting to 16.05 eV and 0.81 eV, respectively. According to the formula ($-E_{HOMO} = 21.22\ eV - E_{cutoff} + E_F$), calculated HOMO level for the NiO_x with and without Br-2PACz were -5.18 eV and -5.98 eV, respectively.

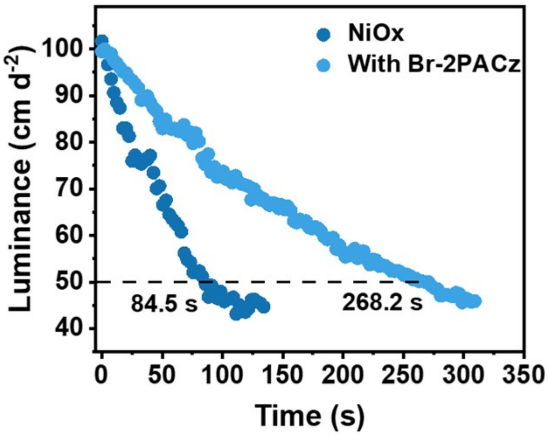

Figure S11. Operational stability (T_{50}) measurement of PeLEDs with NiO_x and Br-2PACz modified NiO_x substrates (initial luminance of 100 cd m^{-2}).

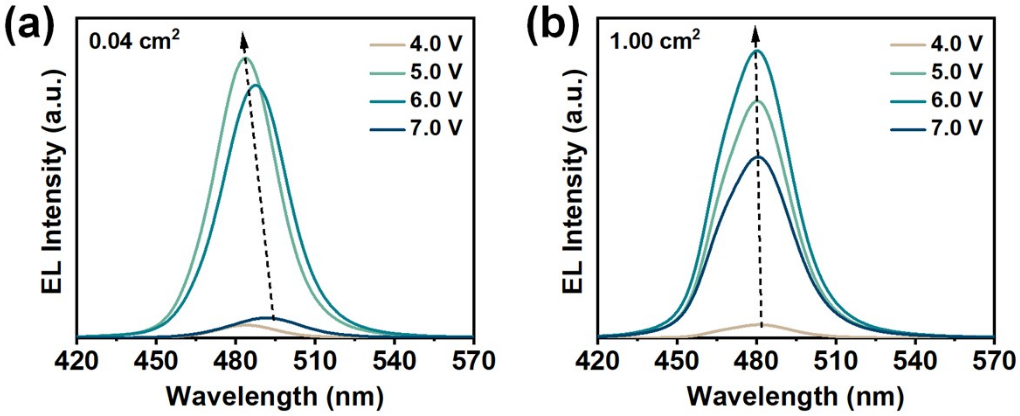

Figure S12. EL spectra of the air-prepared PeLEDs based on a NiO_x substrate, measured at different voltages.

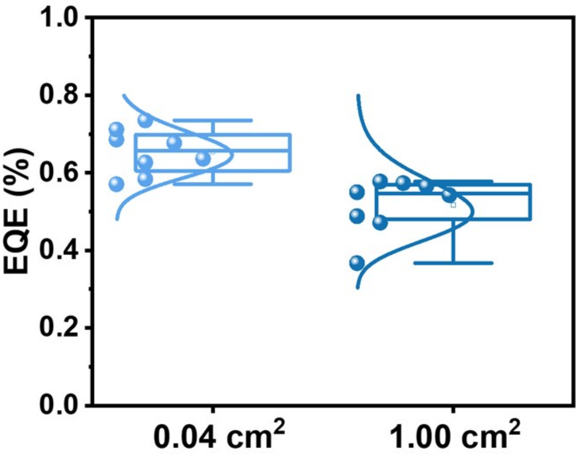

Figure S13. The statistic of EQE of these air-prepared PeLEDs on NiO_x substrate.